Thermochimica Acta, 240 (1994) 129–139
Elsevier Science B.V., Amsterdam
SSDI 0040-6031(94)01705-L

Dynamic evaporation behaviour of diketonate compounds of yttrium, copper and barium

Kan-Sen Chou * and Guan-Jr Tsai

Department of Chemical Engineering, National Tsing Hua University, Hsinchu 30043, Taiwan

(Received 31 August 1993; accepted 19 January 1994)

Abstract

The dynamic evaporations of $Y(thd)_3$, $Cu(thd)_2$ and $Ba(thd)_2$, where thd is 2,2,6,6-tetramethyl-3,5-heptane dionate, were studied using a microbalance technique. Our primary objective here was to investigate the evaporation stability of these compounds with respect to time. Our results showed that the evaporation rates of these compounds decreased inevitably with time due to the decrease in sample weight. The reasons for the decrease in evaporation rate with sample weight are: (i) the decrease in effective surface area with sample weight and (ii) the increase in diffusion distance in the region above the sample within the cell. Our results indicated that by preparing $Cu(thd)_2$ and $Y(thd)_3$ as pellets and then placing them level with the cell rim produces uniform evaporation rates. For $Y(thd)_3$, an additional decrease in evaporation rate occurred at high temperatures due to coalescence between particles and, hence, a decrease in surface area. The evaporation rate of $Ba(thd)_2$ decreased quite significantly with time. An empirical equation of the form $n = n_0(T) + a \exp(-bt)$ fitted our results quite well. There were some oligomers in the original sample, whose quantities seemed to decrease after thermal treatments. A species like $Ba(thd)_2 \cdot Hthd$, may also exist which would make the Ba content in the original sample lower than in pure $Ba(thd)_2$.

INTRODUCTION

The organometallic vapour-phase epitaxy (OMVPE) technique has been successfully applied to the growth of high-temperature superconducting $Y_1Ba_2Cu_3O_{7-x}$ (YBCO) films [1–5]. This technique is capable of growing YBCO films with $T_c \geqslant 90$ K and $J_c \geqslant 10^6$ A cm^{-2} (at 77 K). In spite of these successes, problems in OMVPE still remain to be solved before industrial applications are possible. One such problem relates to the thermal stability of organometallic (OM) precursors as sources of respective metal components and also the reproducibility of their evaporation rates. It is well known that an OMVPE process is composed of four basic steps, i.e. precursor evaporation, vapour transport, decomposition and reaction between these compounds, and incorporation of constituent atoms into solid

* Corresponding author.

films. A controlled and reproducible evaporation behaviour is therefore the first step towards controlled and reproducible film properties, such as chemical compositions.

Of the various tested OM compounds, β-diketonates with thd ligands (thd is 2,2,6,6-tetramethyl-3,5-heptane dionate, $C_{11}H_{19}O_2$) were by far the most frequent choices. Among the diketonates of Y, Cu and Ba, $Ba(thd)_2$ is the most troublesome, exhibiting both chemical and thermal instabilities [6, 7]. This situation may be improved through proper storage [8] or molecular stabilization by forming diketonate complexes [9]. A few other alternatives aiming at all three OM precusors have also been proposed for achieving controlled evaporation behaviours. For example, Hiskes et al. [10] packed the powder mixture of the three OM compounds into a pyrex tube and evaporated it using a steep temperature gradient. Matsuno et al. [11] dissolved these precursors in tetrahydrofuran (THF), and then atomized and thermally evaporated this solution. Sant et al. [12], however, utilized patented special processing equipment for these solid precursors. Regardless of these efforts, it seems that no one has paid attention to the evaporation stability of these compounds with respect to time. It is conceivable that if the evaporation rates of Y, Ba and Cu diketonates vary differently with respect to time, the ratios of individual molecules arriving at the substrate for growth reaction would then vary accordingly. In other words, the film compositions might vary with time and thickness. The objective of this work is therefore to investigate the evaporation dynamics of these OM compounds utilizing the microbalance technique. We hope to determine conditions that can produce stable evaporation for these diketonates. In addition, the nature of the thermal instability of these compounds, especially $Ba(thd)_2$, is discussed.

EXPERIMENTAL

The OM compounds employed in this work were $Cu(thd)_2$, $Y(thd)_3$ and $Ba(thd)_2$ from Strem. Both $Cu(thd)_2$ and $Y(thd)_3$ were supplied in the form of large crystals, which were ground to smaller particles before use. $Ba(thd)_2$ was already a fine powder and was used as received. These powders were stored in Ar and under refrigeration (below 0°C) when not in use.

The dynamic evaporation of these OM precursors was investigated using a Cahn balance (model C2000). The schematics of our set-up is shown in Fig. 1. OM powders of specified weight were placed in a small aluminium cell which was then hung inside a quartz tube. Heating of this quartz tube and our OM sample was provided by a heating tape. A thermocouple was placed as near to the sample cell, without touching it, as possible for temperature control. The flow rates of argon and the system pressure were usually maintained at the levels employed in ordinary OMVPE growth experiments. In a few runs, pellets made from these powder precursors,

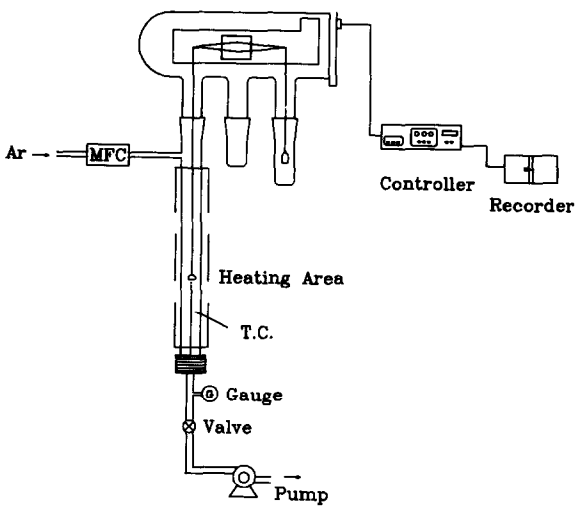

Fig. 1. Schematics of the experimental set-up.

instead of the powder itself, were used to obtain a better control of the evaporation surface area.

To investigate its metal content after thermal treatment, residues of $Ba(thd)_2$ from different temperatures were dissolved in dilute nitric acid and then analysed by the ICP-AES (Plasmakon S-35) technique. The purpose of this work is to provide information on the possible composition of $Ba(thd)_2$ residues after the evaporation process. Mass spectrometry (JEOL SX-102A) was performed on the gaseous products of this compound. In this analysis, OM samples were first dissolved and diluted in tetrahydrofuran and then heated at about 128°C min^{-1} to 350°C. Vapours evolved from the samples were analysed continuously.

RESULTS AND DISCUSSION

Dynamic rates of $Cu(thd)_2$ and $Y(thd)_3$

Figures 2 and 3 show the respective evaporation rates of $Cu(thd)_2$ and $Y(thd)_3$ as a function of time at several different temperatures. All exhibited more or less decreasing trends. The average rates of decrease in evaporation rates, dn/dt, are about 2.1×10^{-8} (130°C) and 5.9×10^{-8} mol h^{-1} min^{-1} (135°C) for $Cu(thd)_2$ and 1.4×10^{-9} (120°C) and 3.2×10^{-9} mol h^{-1} min^{-1} (130°C) for $Y(thd)_3$. Clearly, the higher the evaporation rate, the greater the rate of decrease observed. In the case of $Y(thd)_3$, the initial rate of decrease (say for the first 50 min) in evaporation rates at 135°C seems higher than that for the rest of the experimental period. This is probably caused by coalescence of the particles, accompanied by a corresponding decrease in

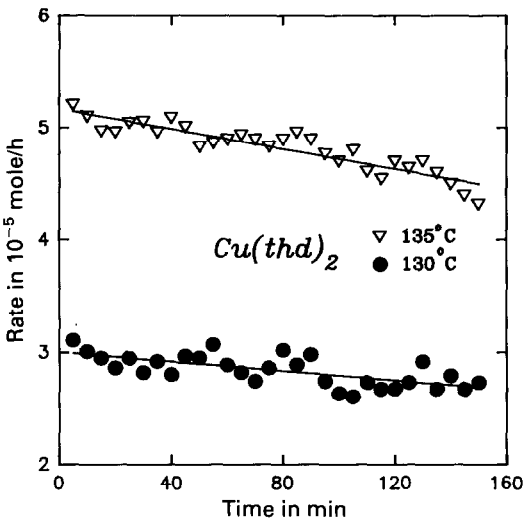

Fig. 2. Variation in evaporation rates of Cu(thd)$_2$ with time; $P = 20$ Torr, $Q = 34.65$ sccm.

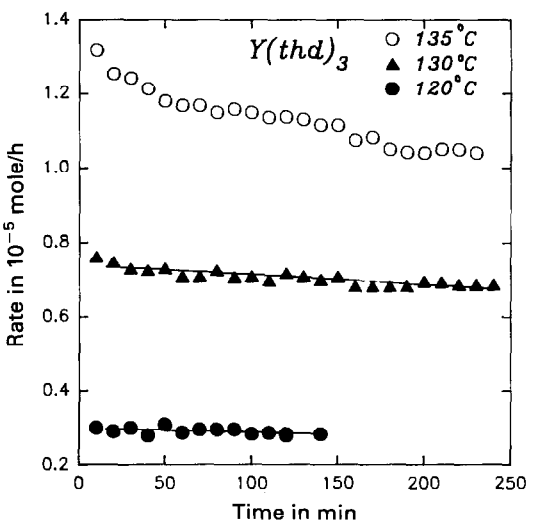

Fig. 3. Variation in evaporation rates of Y(thd)$_3$ with time; $P = 20$ Torr, $Q = 34.65$ sccm.

surface area, during heating at this temperature. The difference in particle morphology before and after heating can be clearly distinguished. This phenomenon was not observed for Cu(thd)$_2$ whose melting temperature is higher than that of Y(thd)$_3$, i.e. 198°C vs. 165–170°C [13]. In other words, this coalescence of particles should also occur for Cu(thd)$_2$ if the temperature is high enough.

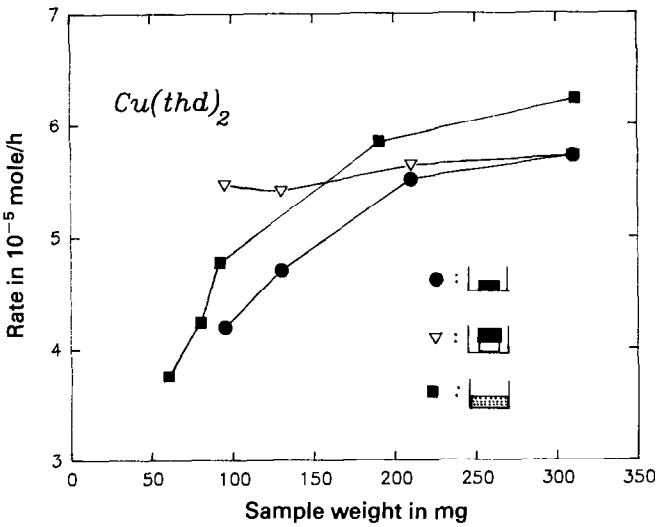

Fig. 4. Changes of evaporation rates with sample weight for $Cu(thd)_2$: ■, as loose powder; ▽, as a pellet, with its surface level with the cell rim; and ●, as a pellet placed directly in the cell ($T = 128°C$, $P = 10$ Torr, $Q = 34.65$ sccm).

Effect of sample weight on evaporation rates of $Cu(thd)_2$ and $Y(thd)_3$

In our previous study on a horizontal evaporator [14], we noticed that the amount of sample in the cell could affect the observed evaporation rates. The same dependency was also found in the present work using a microbalance in which the carrier gas flowed vertically past the cell. Figure 4 shows the evaporation rates of $Cu(thd)_2$ versus their initial weights. These numbers were averages for a 25–30 min experimental period. Three cases are presented here. In the first case, loose powder was laid in the cell. In the second, a pellet of the same weight was placed in the centre of the cell, while in the third case, the pellet was elevated to the same height as the cell, i.e. the surface of the pellet was level with the cell rim. It is obvious from this figure that the changes in rates are more significant for the first two cases than for the third arrangement.

In our previous article [14], we mentioned that the evaporation rates of solid precursors are at least dependent upon: (i) effective surface area of sample, which should be influenced by particle size, state of packing, and, to a lesser degree, sample weight; and (ii) diffusion in the free space (yet still within the cell) above the sample. The results shown in Fig. 4 can now be discussed following the same principle.

(1) Loose powder produced higher evaporation rates than pellets of the same weight due to higher "effective" surface area.

(2) Elevated pellets of different weights showed more uniform evaporation because their surface areas are about the same and all the vapour

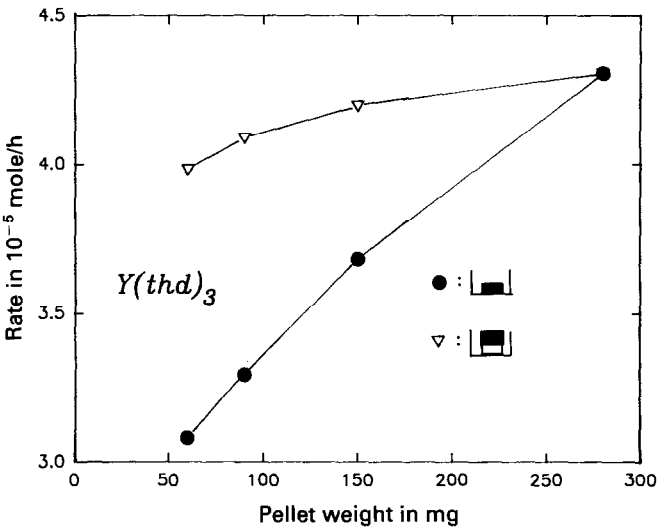

Fig. 5. Changes in evaporation rates of $Y(thd)_3$ with pellet weight, placed either directly in the cell (●) or at an elevated position (▽), as shown ($T = 140°C$, $P = 10$ Torr, $Q = 34.65$ sccm).

molecules could go directly into the carrier gas. If not elevated, vapour molecules from pellets had to diffuse some distance before going into the carrier gas.

(3) Decreases in evaporation rate with sample weight were a combined result of the above two reasons. Wahl et al. [15] also discussed the effect of "filling level" in a sample cell and reported a similar decrease in evaporation rate with less filling. Data for $Y(thd)_3$, shown in Fig. 5, exhibit a similar trend.

The decrease of rate versus time can be explained in terms of a decrease in sample weight during the experiments. The slope of evaporation rate with respect to time can be converted into slope with respect to weight, i.e.

$$dn/dt = (dn/dw)(dw/dt) = (dn/dw)(1/n) \approx (dn/dw)(1/n_{av}) \quad (1)$$

We can then obtain from Fig. 2 a value of about $(1.0–1.7) \times 10^{-7}$ mol h^{-1} mg^{-1} for $Cu(thd)_2$. From Fig. 4, the slope for the loose powder is about 2.1×10^{-7} mol h^{-1} mg^{-1} (for the range 60–100 mg), which is very close to the data calculated from Fig. 2. In other words, we can claim that the observed decrease in evaporation rate with time is entirely due to the decrease in sample weight.

Rates of $Ba(thd)_2$

Decreases in evaporation rates of $Ba(thd)_2$ with time had been reported in the literature, but without any systematic data. Figure 6 shows our results

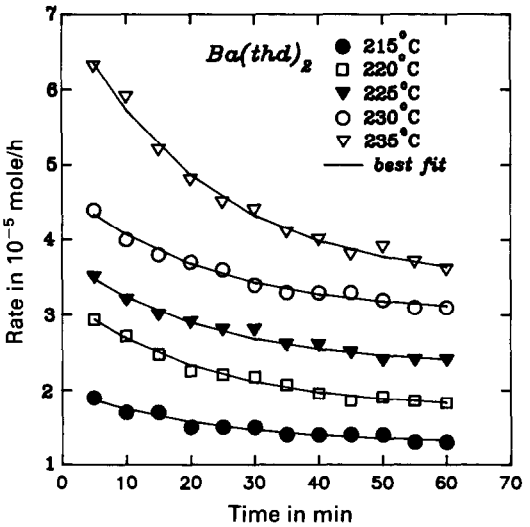

Fig. 6. Evaporation rates of $Ba(thd)_2$ as a function of time; $P = 10$ Torr, $Q = 34.65$ sccm. Curves are drawn based on fitted empirical equations.

for the temperature range from 210 to 235°C. The evaporation rates decrease quite markedly at high temperatures. Nevertheless, the rate seems to reach a steady state value after some time. Because the melting temperature of $Ba(thd)_2$ is only 195–200°C [13], lower than our experimental temperature, this sample should be a melt during evaporation. Therefore, the "surface area" effect is not important here. Moreover, the sample weight was kept at 100 mg for all these runs.

Judging from the shape of these curves, we propose to use the following empirical equation to fit these data

$$n = n_0(T) + a \exp(-bt) \tag{2}$$

where $n_0(T)$ may be considered as the steady state evaporation rate of the principal species in $Ba(thd)_2$ at temperature T and the second term is a contribution from some impurity species. This impurity is present in only a limited amount and therefore its contribution decreases with time until it is totally consumed. The best-fitted values are $b = 0.047$ (min^{-1}) and a in the range from 0.75×10^{-5} to 3.7×10^{-5} (mol h^{-1}), reflecting variable amounts of impurity species in the tested samples. The fittings, shown as solid curves in Fig. 6, are in good agreement with our data. Figure 7 shows the Arrhenius plot of $n_0(T)$ which can be expressed as

$$n_0(T) \text{ mol h}^{-1} = 7.17 \times 10^5 \exp(-24000 \text{ cal mol}^{-1}(RT)^{-1}) \tag{3}$$

The apparent heat of evaporation is found to be 24 kcal mol^{-1}, which is close to the value 23.4 kcal mol^{-1} given by Schmaderer et al. [1].

Figure 8 shows the Ba contents in the heated samples. The "new" sample refers to a new purchase from Strem, while the "old" sample was a previous

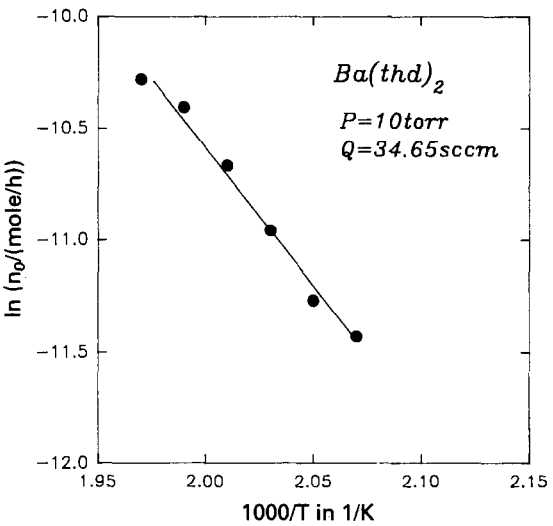

Fig. 7. Arrhenius plot of $n_0(T)$ versus $1/T$ for $Ba(thd)_2$.

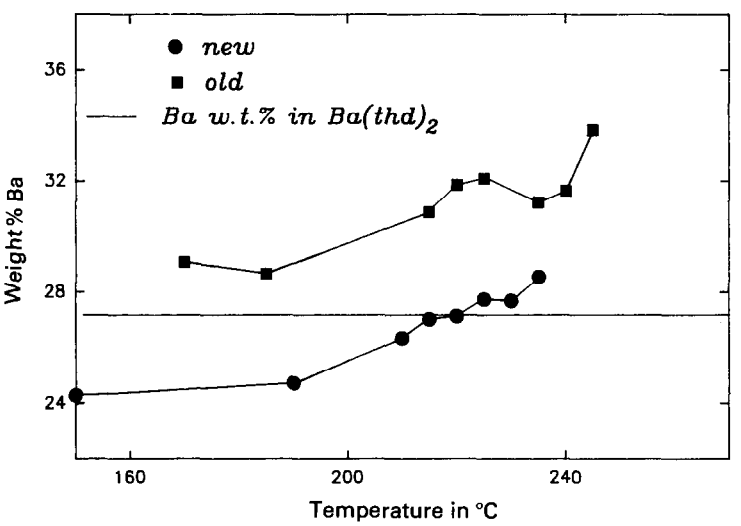

Fig. 8. Barium contents in two batches of $Ba(thd)_2$ samples after being heated to various temperatures for 1 h.

purchase. The theoretical Ba contents (as wt.%) in $Ba(thd)_2$, $BaCO_3$, $Ba(OH)_2$ and BaO are 27.3, 69.6, 80.2 and 89.6% respectively. Several comments can now be made with regards to these data.

(1) The Ba content always increases upon heating, indicating that some of the $Ba(thd)_2$ is converted to inorganic Ba compounds via some solid-state reaction. If we assume the decomposition product is $BaCO_3$, we can then calculate the contents of $BaCO_3$ in the residue from 235°C, for the "new"

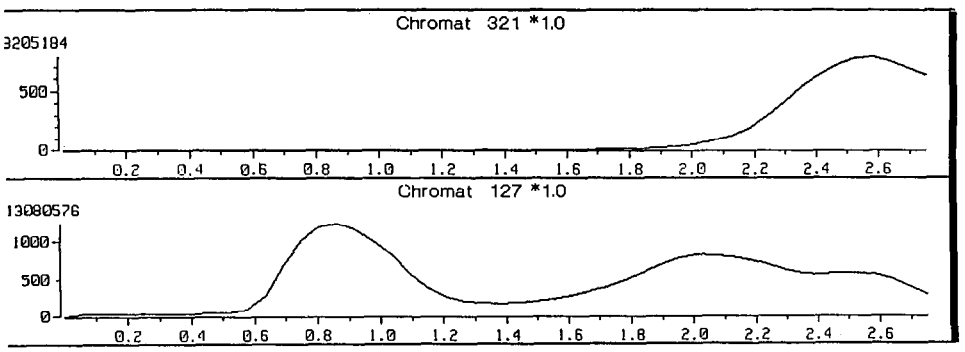

Fig. 9. Mass spectra of m/z 321 (upper) and m/z 127 (lower) peaks as a function of time (which is equivalent to temperature).

sample treated for 1 h to be around 3.3 wt.% only. This may be taken as negligible. In general, "old" samples, probably due to improper storage, contained higher inorganic Ba compounds than the corresponding "new" samples. The highest Ba content was observed for the "old" sample treated at 245°C. Here we calculate the $BaCO_3$ in the residue to be about 15.8 wt.%.

(2) The 150–210°C heated "new" $Ba(thd)_2$ samples showed Ba contents lower than the theoretical 27.3 wt.% value. This implies that the Ba-containing species has a higher molecular weight than $Ba(thd)_2$, e.g. $Ba(thd)_2 \cdot Hthd$ (or as $H[Ba(thd)_3]$) complex. Turnipseed et al. [16] mentioned a similar complex for $H[Ba(fod)_3]$. Figure 9 shows the MS of the 127 m/z (a fragment from thd) and 321 m/z (a fragment from $Ba(thd)_2$) species recorded versus time (equivalent to temperature). The first 127 m/z signal may correspond to the evaporation of free solvent in our sample; the second is considered to be released from $Ba(thd)_2 \cdot Hthd$, and the third is derived from $Ba(thd)_2$ itself. The 321 m/z signal appearing at about the same temperature as the third peak of the 127 m/z species may serve as additional evidence for this.

Finally, Fig. 10 shows MS spectra of several samples. It is very clear that the dimer and trimer of $Ba(thd)_2$ are present in the original sample. To our surprise, the peaks corresponding to these oligomers disappear or weaken after thermal treatment. In THF-refluxed samples, peaks corresponding to the dimer are barely detected. We speculate that these oligomers may "dissociate" into momomers upon heating or refluxing with solvent such as THF. However, further studies are required to fully illustrate the chemistry associated with the evaporation of $Ba(thd)_2$ compound.

CONCLUSIONS

Based on the results reported here, we can conclude that the evaporation process for $Y(thd)_3$ and $Cu(thd)_2$ is strongly influenced by their effective surface areas and the distance that vapour molecules have to diffuse before

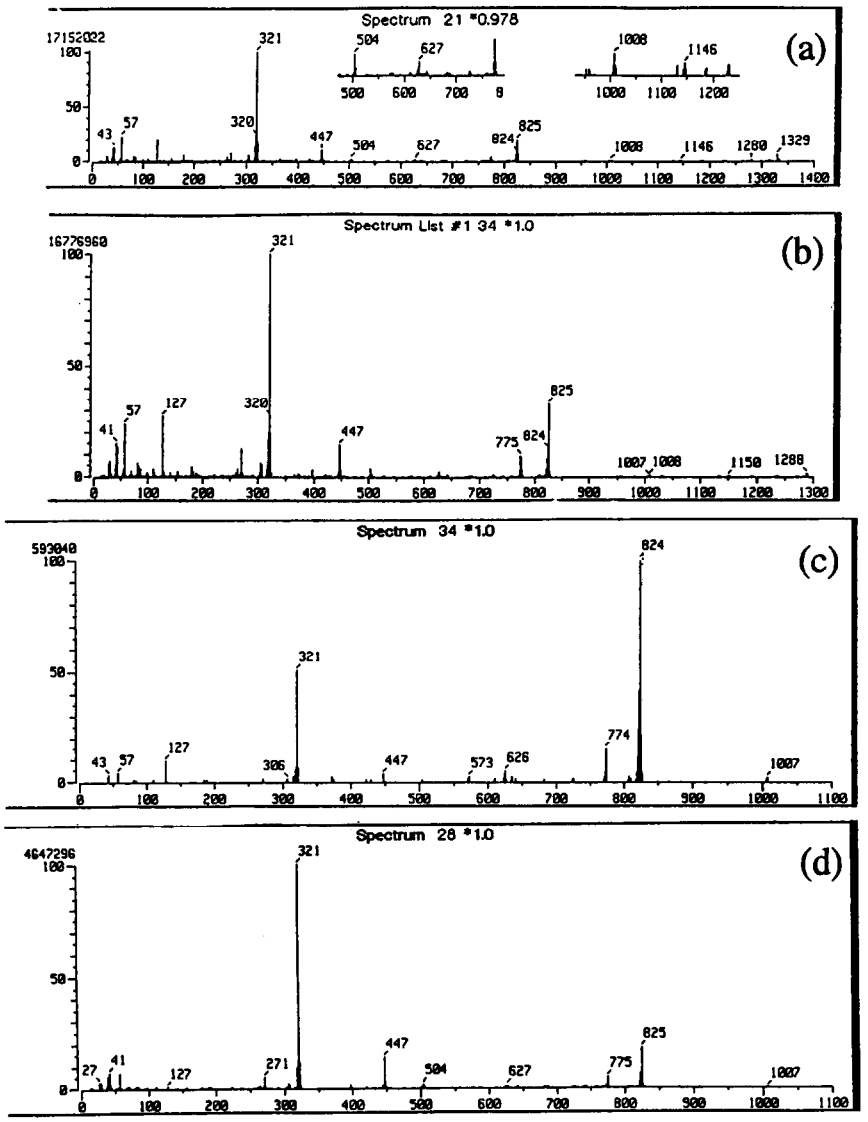

Fig. 10. Mass spectra of $Ba(thd)_2$ after different treatments: (a) original sample; (b) heated at 150°C for 1 h; (c) heated at 230°C for 1 h; and (d) refluxed in THF at 50°C for 10 h.

going into the carrier gas. Our experience suggests that it is best to prepare these samples in pellet form and to place the pellet level with the cell rim in order to produce uniform evaporation rates. The evaporation rate of $Ba(thd)_2$ is also influenced by the composition of the starting material which then depends upon its history and storage. Oligomers and also $Ba(thd)_2 \cdot Hthd$ may exist in the original sample. However, the amounts of oligomers present seem to decrease after thermal treatment or refluxing with THF. The time variation of the evaporation rates of $Ba(thd)_2$ can be fitted

by the equation $n = n_0(T) + a \exp(-0.047t)$. The apparent heat of evaporation process calculated from $n_0(T)$ gave a value of 24 kcal mol^{-1}, which is in good agreement with literature data [1] determined by a different technique. By analysing the Ba content in the residues after heat treatment, it was found that $Ba(thd)_2$ starts to decompose via some solid-state reaction at temperatures above 200°C.

ACKNOWLEDGEMENT

The authors thank National Science Council of ROC for financial support of this research work (Grant No. NSC82-0511-M 007-143).

REFERENCES

1 F. Schmaderer, R. Huber, H. Oetzmann and G. Wahl, Appl. Surf. Sci., 46 (1990) 53–60.
2 T. Hirai and H. Yamane, J. Crystal Growth, 107 (1991) 683–691.
3 K. Higashiyama, T. Ushida, H. Higa, I. Hirabayashi and S. Tanaka, Jpn. J. Appl. Phys., 30(6) (1991) 1209–1215.
4 A. Feng, L. Chen, T.W. Piazza, H. Li, A.E. Kaloyeros, D.W. Hazelton, L. Luo and R.C. Dye, Appl. Phys. Lett., 59(10) (1991) 1248–1250.
5 W.J. DeSisto, R.L. Henry, H.S. Newman, M.S. Osofsky and V.C. Cestone, Appl. Phys. Lett., 60(23) (1992) 2926–2928.
6 H. Harima, H. Ohnishi, K. Hanaoka, K. Tachibana and Y. Goto, Jpn. J. Appl. Phys., 30(9a) (1991) 1946–1955.
7 R. Sato, K. Takahashi, M. Yoshino, H. Kato and S. Ohshima, Jpn. J. Appl. Phys., 32(part 1, no. 4) (1993) 1590–1594.
8 T. Hashimoto, H. Koinuma, M. Nakabayashi, T. Shiraishi, Y. Suemune and T. Yamamoto, J. Mater. Res., 7(6) (1992) 1336–1340.
9 W.S. Rees, C.R. Caballero and W. Hesse, Angew. Chem. Int. Ed. Engl., 31(6) (1992) 735–737.
10 R. Hiskes, S.A. DiCarolis, J.L. Young, S.S. Laderman, R.D. Jacowitz and R.C. Taber, Appl. Phys. Lett., 59(5) (1991) 606–607.
11 S. Matsuno, F. Uchikawa, S. Utsunomiya and S. Nakabayashi, Appl. Phys. Lett., 60(19) (1992) 2427–2429.
12 C. Sant, P. Gibart, P. Genou and C. Verie, J. Crystal Growth, 124 (1992) 690–696.
13 Material safety data sheet, Strem Co., Newburyport, MA, USA, 1991.
14 K.S. Chou, M.J. Huang and M.Y. Shu, Thermochim. Acta, 233 (1994) 141–152.
15 G. Wahl, W. Decker, M. Pulver, R. Stolle, O.Y. Gorbenko, A.R. Kaul, Y.Y. Erokhin, I.E. Graboy, M. Sommer and U. Vogt, Physica C, 209 (1993) 195–198.
16 S.B. Turnipseed, R.M. Barkley and R.E. Sievers, Inorg. Chem., 30 (1991) 1164–1170.